Proceedings of 2004 IEEE/RSJ International Conference on
Intelligent Robots and Systems
September 28 - October 2, 2004, Sendai, Japan

Visually-Guided Protein Crystal Manipulation Using Micromachined Silicon Tools

Atanas Georgiev, Peter K. Allen
Department of Computer Science
Columbia University, New York, NY 10027
{atanas,allen}@cs.columbia.edu

William Edstrom
Department of Biological Sciences
Columbia University, New York, NY 10027
edstrom@biology.columbia.edu

Abstract— **We present a system for protein crystal micromanipulation with focus on automated crystal mounting for the purposes of X-ray data collection. The system features a set of newly designed micropositioner end-effectors we call microshovels which address some limitations of the traditional cryogenic loops. We have used micro-electrical mechanical system (MEMS) techniques to design and manufacture various shapes and quantities of microshovels. Visual feedback from a camera mounted on the microscope is used to control the micropositioner as it lowers a microshovel into the liquid containing the crystals and approaches a selected crystal for pickup. We present experimental results that illustrate the applicability of our approach.**

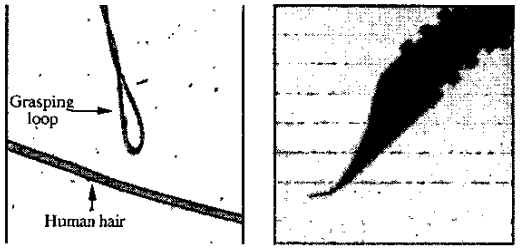

Fig. 1. Mounting Tools: (a) A cryogenic loop: (b) a microshovel.

I. Introduction

The completion of the human genome has led to a shift in biologists' focus toward proteins, the product of genes. A large coordinated effort is under way worldwide to master the process of determining the 3-D atomic-level structure of proteins [1]. These experimentally determined structures can be combined with the sequence data using bioinformatics methods to produce structural coverage of the majority of proteins. This is expected to have a significant impact on biological and medical research by shedding light on the relationships of structure to function and disease, directing structure-based drug design [2] and refining our understanding of evolutionary relationships between proteins.

The structure determination effort centers on developing the capability of processing proteins on a large scale — a high-throughput pipeline starting from producing the proteins and leading through various stages to the eventual discovery of the spatial arrangement of the protein atoms. This necessitates the development of strategies and tools for automated and fast manipulation of protein crystals, as one of the most popular methods for structure determination is X-ray crystallography [3].

Automated protein crystal manipulation is a challenging task because of the unique combination of factors involved. Protein crystals are small (sizes of interest are between 25 and $1000\mu m$) and fragile. They are also sensitive to environmental variations, especially temperature. Their growth environment is a $0.1\text{-}5\mu l$ droplet of liquid which dehydrates in a matter of minutes once exposed to room conditions. Classical strategies of manipulation will not work at these scales due to the required precision (beyond the calibration range of conventional industrial precision devices) and additional problems related to microscale phenomena. Currently, the mechanics of micromanipulation is poorly understood and thus results of sensorless micromanipulation strategies are unpredictable. Obtaining reliable feedback is also problematic.

Our work is aimed at using computer vision to provide the compliance and robustness which precise crystal manipulation requires without the need for extensive analysis of the physics of grasping or a detailed knowledge of the environment. The specific task we are interested in is known as *crystal mounting* and consists of picking an individual protein crystal from its growth solution for the purpose of X-ray data collection. This task is currently performed manually by skilled crystallographers using a tool called *a cryogenic loop* (Figure 1a). It is a loop made of a thin ($10\mu m$ or $20\mu m$) thread of nylon glued to the tip of a metal pin. Mounting a target crystal on the loop requires time, patience and excellent motor skills.

In a previous work [4], we proposed an integrated control system, consisting of a high-resolution optical microscope, digital imaging system, image based servo-controllers and a micromanipulator for precise positioning of a cryogenic loop with respect to a crystal. Here, we extend that work by presenting a different method for crystal mounting based on a novel kind of tool, *a microshovel* (Figure 1b), which we have designed to address certain shortcomings of the loops. We have also improved and adapted our previous visual servoing method to the peculiarities of the microshovels.

The remainder of this paper is organized as follows: After a brief review of the related work, we describe our hardware setup and the task at hand in Section III. In Section IV, we present the our new tools for crystal mounting.

0-7803-8463-6/04/$20.00 ©2004 IEEE

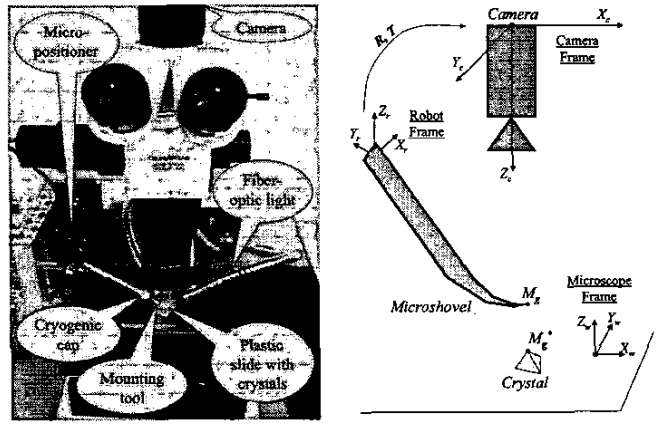

Fig. 2. Setup: (a) workstation for protein crystals manipulation: (b) coordinate frames.

The following two sections describe improvements we have made to our visual servoing methods and their adaptation to the specifics of the microshovels. Experimental results are presented in Section VII.

II. Related Work

One of the major advances in robotics over the last 20 years is the visual control of robotic manipulators [5]. The advent of fast and inexpensive digital imaging technology has allowed camera systems to be integrated as part of a closed-loop feedback control system [6]. Visual servoing strategies have been successfully implemented at the microscale level for manipulation of known micro-electromechanical systems with calibrated devices [7], [8]. Visual servoing has also been successfully used for biological cell injection [9].

Visual servoing is classified into two main approaches [5], [10], [11]. The first one [12], [13], based on the computation of a 3-D Cartesian error, requires a perfect CAD-model of the object and a calibrated camera to obtain unbiased pose estimation. In the second approach, the pose estimation is omitted and the control loop is directly closed in the image space. That ensures local convergence and stability in presence of modeling errors and noise perturbations [14]. In our case, the models of the observed targets are unknown and the system is not calibrated. We thus use the image-based approach.

In terms of the mechanics of the actual manipulation, quite a few very diverse ideas have been pursued. Various kinds of microgrippers have been proposed [15]. Optical trapping by a laser has been successfully used for both direct and indirect cell manipulation [16]. A micromanipulation tool based on adhesive forces has been demonstrated [17]. Methods exploiting magnetic and electrostatic forces are also being used.

Unfortunately, not many of these approaches can be easily applied to our case. Microgrippers pose the risk of structural damage to the fragile crystals. Optical trapping has the potential to damage the crystals because of excessive heat. Adhesive forces can not be relied upon because of the drastic variations of the composition of the protein crystals and their environments. Dielectrophoresis actuates all objects within the electromagnetic field making it difficult to isolate an individual target.

These considerations have led us to settle on a microshovel design which is thin enough to be able to easily slide under a crystal and wide enough to provide a support base on which the crystal rests as it is extracted from the liquid thus minimizing the chance of breaking its structural integrity.

III. Setup and Task Description

Our workstation (see Figure 2a) is centered around a Sutter MP-285 micropositioner with three degrees of freedom — independent motion control along the X, Y and Z axes. This positioner has a resolution of 40 nm. A crystal mounting tool (e.g. a cryogenic loop or a microshovel) is attached as the manipulator end-effector. The tool and the protein crystals are observed through an Olympus SZX12 optical microscope (eye-to-hand configuration [18]). The microscope provides a total magnification from 8.4x to 108x and has a CCD camera adapter onto which a Sony XC-77 camera is mounted. The camera and the micropositioner are connected to a PC which processes the visual feedback and controls the micropositioner.

At the beginning of the procedure, the user places a plastic slide with the droplet containing the protein crystals on the microscope tray such that they are in the field of view. The microscope is adjusted so that the crystals are in focus. The tooltip is in the field of view, however, above the liquid and, therefore, out of focus because of the short depth of field at the nominal magnification levels. The user specifies a target crystal by selecting a rectangular region of interest (ROI) on the screen and the process starts.

Let $\mathcal{F}_c$ and $\mathcal{F}_r$ be the camera frame and the robot frame respectively (Figure 2b). We assume that the Z-axis of the camera frame and of the Z-axis of the robot control frame are parallel. Our goal is to approach the crystal

with the tool, slide the tool under the crystal and lift up the crystal. To approach the crystal, we need to minimize the distance between the microshovel with coordinates $\mathbf{M}_c = [X_c, Y_c, Z_c]^T$ in $\mathcal{F}_c$ and the target crystal ROI $\mathcal{M}^*$ with coordinates $\mathbf{X}_c^* = [X_c^*, Y_c^*, Z_c^*]^T$ in $\mathcal{F}_c$.

There are obviously three degrees of freedom that must be controlled. We have split the task into two phases: a vertical descent and a horizontal approach to the target. The purpose of the vertical descent phase is to penetrate the liquid, bring the tool into focus and at the appropriate depth for pickup, and detect its position in the field of view. The horizontal motion is used for the actual approach and pickup of the crystal. The robot motion along the X and Y axes is controlled by minimizing the distance between the tool and the crystal in image space. The detail of these two phases are discussed after we describe the microshovels.

IV. Tools For Protein Crystal Mounting

The cryogenic loop (Figure 1a) is currently the crystallographers' tool of choice for crystal mounting and X-ray data collection. It has a number of unique properties that make it suitable for the task: It is soft and flexible, which protects it from being easily broken. It is minimalistic and open, which allows one to easily detect if there is a crystal within it. When a crystal is lassoed in the loop, surface tension forces work to keep it in place by nicely wrapping the nylon thread around it.

In the context of automated crystal mounting, however, loops pose certain problems which stem mainly from their flexibility. We have been exploring the idea of sliding a loop under the target crystal to lasso it. While our experience shows that this is certainly possible, in practice, it is not very robust. First, during crystallization, some protein crystals tend to attach themselves to the bottom as if glued. If the loop encounters such a crystal, it will most likely bend because it is less rigid than the crystal. In such situations, crystallographers first use rigid metallic micro-tools to dislodge the crystal before they proceed with mounting. This is a delicate procedure because it is important that the fragile crystal remains intact. Second, even if the crystal is free-floating, the loop may simply start pushing it, instead of sliding underneath. This is often the case with smaller crystals in non-viscous fluids. Manually, one would use rotational degrees of freedom to perform a "scooping" move and lasso the crystal with the loop. This is not easily imitated programmatically. Finally, tracking a deformable object by using visual feedback is challenging.

For these reasons, we decided to look at alternatives to cryogenic loops. Two questions regarding a possible substitute are: What will it be made of and what kind of shape should it have? In terms of shape, we pursued our idea of being able to slide the tool under the crystal to lift it up. That leads to a shape that has a large flat tip. In terms of material, we had to consider additional constraints imposed by the process. The next step of the protein crystal pipeline is to take X-ray diffractograms of the crystal which, after some analysis, reveal the needed 3-D structure. Since the manipulation tool is to be used on the X-ray diffractometer, it is important that the tool's diffraction pattern does not interfere with the one of the crystal so that its effects can be later filtered out of the diffractogram.

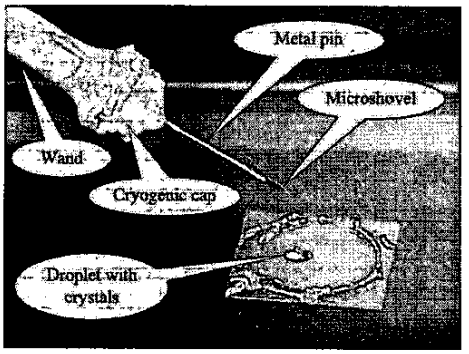

Fig. 3. A close-up showing a microshovel glued to the metal pin of a cryogenic cap which is attached to a wand held by the micropositioner.

As candidates for our shovel, we tested seven different materials on the X-ray diffractometer — aluminum, brass, copper, silicon and three types of plastic. With the exception of the silicon, the other materials are readily available as thin sheets of shim stock — we looked at thicknesses of $25\mu m$ or thinner. We found that the only candidate that has no interfering diffractions is silicon.

Existing MEMS techniques allow us to design shapes, draw photomasks and create tools with high precision out of silicon wafers. We have designed and produced 30 distinct shapes and sizes of silicon microshovels which have been used for the rest of the experiments and methods in this paper (Figure 1b). The size of the tools is about $8mm$ in length, $0.3mm$ in width and $0.7mm$ in thickness, while their tips range between 50 and $279\mu m$ in length and between 7 and $40\mu m$ in height. Each microshovel is marked with a series of notches near its tip which encode in binary its shape and size for easy recognition by a naked eye. The microshovels are prepared for use just as loops are: they are glued to a metal pin attached to a cryogenic cap. The cap itself is designed to easily attach to and detach from a wand held by the micropositioner (Figure 3).

V. Descent

The first phase of the mounting process is to lower the tool into the liquid. The difficulty in this phase is to make sure that the microshovel is exactly at the correct depth — we want it to be just above the bottom (the surface of the plastic slide) so it can move freely. If it is higher than that, sliding under the crystal will be difficult as the shovel may start pushing it instead. If it goes too deep, the sharp front edge of the microshovel will penetrate the plastic slide and the micropositioner will move the whole slide along with the tool. If an attempt is made to move farther down, the force on the tooltip may become too strong and it may break.

Our solution to this is based on the following observation: When the microshovel touches the slide in its

downward motion and starts exerting force, it moves the plastic sliding it along the microscope tray. Since only a small portion of the slide is in the field of view, the motion affects the entire image (as if the camera is moving to the left). This is only valid for a small range of depths (about $500\mu m$), before the tool presses too strongly. The horizontal motion of the slide is in the order of microns, however, under the magnification of the microscope, this translates into motion of tens of pixels and is therefore detectable with computer vision techniques.

Our method consists of moving the microshovel down in small steps (say $100\mu m$) and trying to detect the horizontal motion. After each step, the optical flow between the previous and the current view is computed. This is done using the normalized SSD metric on a grid of uniformly distributed sample points P_i, $i \in [1, N]$. We sample only the right half of the image to avoid large effects of the tool itself. If $\mathbf{d_i}$ is the displacement vector of the sample point P_i, then

$$\bar{\mathbf{d}} = \sum_{i=1}^{N} \mathbf{d_i} \qquad (1)$$

gives us the average flow vector. When the magnitude of the vector is larger than a threshold, we determine that we have reached into the plastic. The threshold is about 1–2 pixels and accounts for small oscillations in the tracking of the sample points between the frames. If no consistent flow has been detected, we continue with another step down until we have a positive contact identification.

At this stage, the tool is in contact with the plastic and needs to be retracted so it can move freely horizontally. Thus, we initiate a similar process as above, only this time moving up and at much finer steps (about $1\mu m$). After each step up, a small horizontal step is made and the optical flow is computed to detect this motion in the image. If it is present, this means that the tool is still in contact with the plastic and we continue moving up. When no horizontal motion is detected, the microshovel is positioned at the correct depth. This also means that it is already in focus.

VI. Approaching and Picking the Crystal

After the microshovel has been lowered to the level of the crystals, horizontal motion is used to approach the target. Two SSD trackers [19] are initialized to initiate the visual servo. The first tracker is initialized manually by the crystallographer with the selected crystal for mounting. The location of the crystal is considered to be the center of the selected rectangle. The second tracker, which follows the microshovel, is obtained by image analysis (Figure 4). After the descent, the tool is slowly moved to the left (at the same depth) until it leaves the image. The moment when the tool is no longer visible is easily recognizable by monitoring the intensity differences of two consecutive frames — once the shovel leaves the field of view, the difference is only due to noise and becomes negligible. At this point a reference image I_0 is taken and the tool is moved back to where it was after the descent phase. A second image I_1 is taken and the difference $dI = I_1 - I_0$

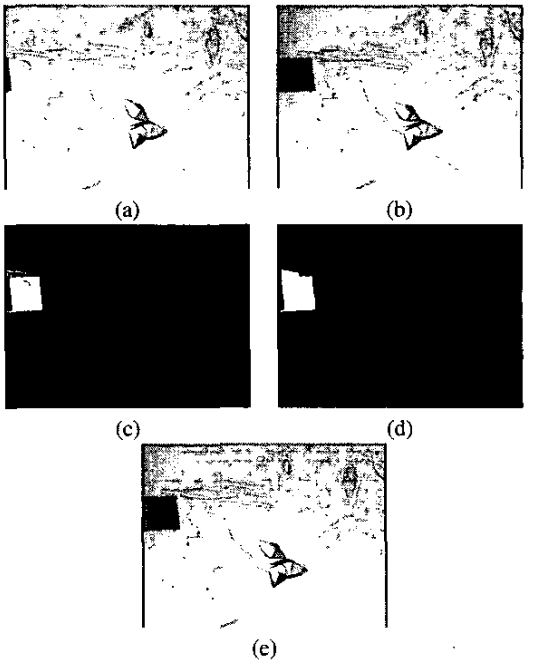

Fig. 4. Detection of the microshovel: (a) The microshovel is moved out of view after the descent phase; (b) The microshovel is moved back where it was after the descent phase; (c) The thresholded image difference between the two images; (d) The result after morphological closure; (e) The identified ROI of the microshovel.

contains a large discrepancy in the area where the tooltip is in I_1. To filter out various other artifacts, we first threshold dI (Figure 4c) and then apply a morphological closure operator (Figure 4d). This has the effect of eliminating small blobs of noise and bridging small gaps in the large blobs. The largest remaining blob is the tooltip itself — we initialize the second tracker with the smallest rectangle containing that blob (Figure 4e).

The visual servoing algorithm tries to align the midpoint of the right edge of the tool ROI with the midpoint of the left edge of the ROI of the crystal. In other words, visual guidance is used to position the tool just in front of the crystal.

Central to the servoing is the image Jacobian $\mathbf{L}$ (also called interaction matrix) which relates the differential motion $\mathbf{ds}$ of an image feature $\mathbf{s}$ to the differential motion in the camera coordinates $\mathbf{dP}$: $\mathbf{ds} = \mathbf{LdP}$. Considering only a planar horizontal motion, the eye-to-hand Jacobian relationship for a single feature point is:

$$\dot{\mathbf{x}} = \mathbf{L}_{xy}\mathbf{R}_{xy}\begin{bmatrix} {}^{r}V_x \\ {}^{r}Vy \end{bmatrix} = \mathbf{L}_{txy}\,{}^{r}\mathbf{V}_{xy} \qquad (2)$$

where $\mathbf{L}_{txy} = \alpha\mathbf{R}_{xy}$ is the eye-to-hand interaction matrix, α is the magnification factor, and $\mathbf{R}_{xy}$ is a 2×2 rotation matrix that maps the control vector expressed in the camera frame ${}^{c}\mathbf{V}_{xy}$ to the control vector expressed in the robot control frame ${}^{r}\mathbf{V}_{xy}$. A suitable control law to make the error vector $\mathbf{e} = \mathbf{x} - \mathbf{x}^*$ decrease exponentially (i.e, $\dot{\mathbf{e}} =$

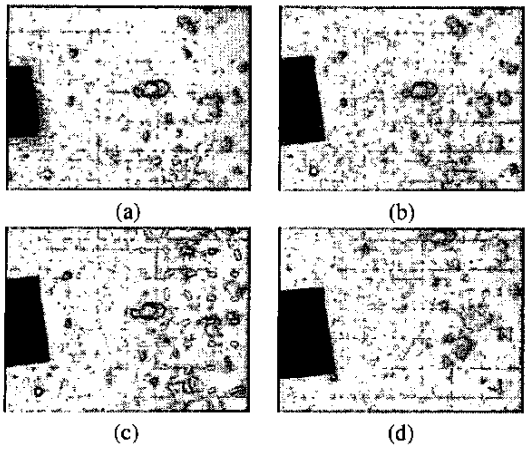

Fig. 5. A descent phase: (a) The initial configuration — the tooltip is high above the liquid and is out of focus; (b) The tooltip has descended into the liquid and is one step before reaching the bottom; (c) The last step is made and the plastic slide has moved. The needles show the optical flow; (d) The final position, after the tooltip has retreated enough to be able to move freely.

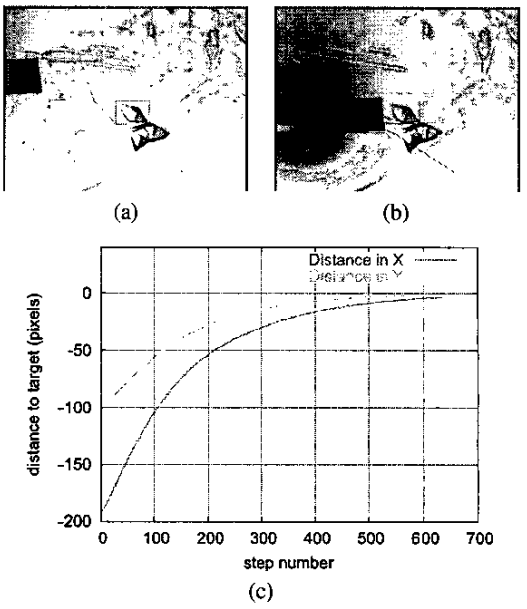

Fig. 6. A visual servo phase: (a) The initial configuration — the tooltip and the target crystals along with the ROI of the two trackers; (b) The microshovel has approached the crystal; (c) A graph showing the convergence of the reference positions of the microshovel and the crystal.

$-\beta$e) to 0 is given by:

$$^{r}\mathbf{V}_{xy} = -\beta\widehat{\mathbf{L}}^{+}_{txy}(\mathbf{x} - \mathbf{x}^{*}) \qquad (3)$$

where $\mathbf{x}^{*}$ is the desired position of the microshovel in image space, $\widehat{\mathbf{L}}_{txy}$ is the estimated image Jacobian and β is a proportional gain.

Judging from a stability study, we fix $\widehat{\mathbf{L}}_{xy} = \hat{\alpha}\widehat{\mathbf{R}}$ to a constant value while ensuring the convergence of control. For our application, $\hat{\alpha}$ is fixed to the value given by the manufacturer. The estimated rotation matrix $\widehat{\mathbf{R}}_{xy}$ is fixed as the closest rotation matrix to $\frac{1}{\hat{\alpha}}\widehat{\mathbf{L}}^{0}_{xy}$ where $\widehat{\mathbf{L}}^{0}_{xy}$ is the interaction matrix numerically computed off-line by observing the repercussion of the robot motion in the image space. Further details can be found in [20].

When the microshovel is positioned just before the crystal, a one-step move command is executed by the micropositioner in the direction of the crystal and of length — the size of the crystal ROI. This is the actual pick-up: the shovel slides under the crystal. It is executed as a single command to avoid the jerkiness caused by the change in acceleration of the micropositioner between two consecutive commands. There is no visual feedback used at this stage yet because the transparent crystal is difficult to spot once on the shovel. Lastly, the microshovel with the crystal on it are slowly raised up above the level of the liquid — the task is completed.

VII. Experiments

To verify the methods described here, we have performed extensive tests of each of the phases as well as the system as a whole. In this section, we show an example run of each phase. All of these experiments have been run on real crystals under the same conditions as crystallographers'.

The first example demonstrates a descent of a microshovel into the liquid (Figure 5). Figure 5a shows the initial configuration before the phase began: The tooltip is well above the liquid and out of focus. It is, however, still possible to tell that it is in the field of view. After the program was started, the tooltip moved down in steps of $100\mu m$ according to the method described in Section V. Figure 5c shows the first frame when the contact with the plastic slide was detected and Figure 5b was the immediately preceding frame. The needles on Figure 5c show the computed optical flow for the sample points. At this stage, the tool started moving up in steps of $2\mu m$ and testing whether it can freely move horizontally. Figure 5d shows the frame when free motion was detected, i.e. the microshovel was at the correct depth.

The second example demonstrates the horizontal visual servoing phase. Figure 6a shows the initial configuration in which the tooltip is at the correct depth. The rectangles around the tool and the crystal are the initial regions of interest for the two trackers. The program for horizontal approach moved the tool toward the crystal while simultaneously tracking both. Figure 6b shows the end result of the visual servoing where the microshovel is just in front of the crystal. The graph in Figure 6c shows how the distance in X and Y of the locations of the two tracked objects exponentially approaches zero with each iteration. Note that at the end both distances are zero, because the reference point of the tool is on the right side of its ROI and the one of the crystal is on the left side. This is because, we are only interested in using servoing up to the point just before pickup takes place.

Finally, Figure 7 shows a successful crystal mounting task executed. Figure 7a, captures the tooltip just after

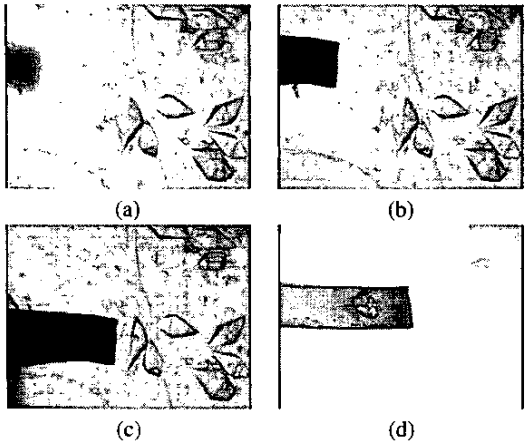

Fig. 7. A complete crystal mounting experiment: (a) The initial condition (b) The microshovel after the descent phase: (c) The microshovel after the approach phase: (d) The microshovel has slid under the crystal and raised it up above the liquid.

the descent phase. Figure 7b is the state after the crystal approach is completed. In Figure 7c, the microshovel has slid under the crystal and lifted it up above the liquid.

VIII. Conclusion and Future Work

We have presented a functional robotic system for protein crystal manipulation based on a micropositioner, an optical microscope with a CCD camera for visual feedback, and software control through a PC. The system features a set of newly designed micropositioner end-effectors which address some limitations of the traditional cryogenic loops. These microshovels have been manufactured in various shapes and sizes using MEMS technology. They are made of silicon, which we have tested for compatibility with the X-ray data collection process. We also presented a number of computer vision and robotics techniques that allow us to detect the microshovels in the visual feed from the camera, lower the tools to the correct depth, track both the microshovel tips and a target crystal, visually servo toward the crystal to pick it up.

One of the most likely reasons for failure of our system is the lack of feedback during the actual pickup phase. This is mainly due to the poor visibility of the crystal at this stage. We are working on improving the lighting conditions so that the crystal remains visible even during pickup and lifting. In this paper, we have assumed that the target crystal has been identified in advance and positioned in the field of view. In practice, this is not always the case and crystal detection and isolation are examples of related problems which we are also working to address.

Acknowledgment

The authors wish to thank Prof. John Hunt and Prof. Liang Tong from the Biological Sciences Department at Columbia University for their help with crystallography, and Prof. Luc Frechette, Akilesh Sridharan, and Dean Moudrukas from the Department of Mechanical Engineering at Columbia University for their assistance with MEMS technology. This work was supported by a grant to the Northeast Structural Genomics Consortium from the Protein Structure Initiative of the National Institute of Health (P50 GM62413).

References

[1] (2004) The protein structure initiative. [Online]. Available: http://www.nigms.nih.gov/psi

[2] C. L. Verlinde, "Structure-based drug design: progress, results and challenges," *Structure 2*, pp. 577–587, 1994.

[3] V. L. Niennaber, P. Richardson, V. Klighover, J. Bouska, V. L. Giranda, and J. Geer, "Discovering novel ligands for macromolecules using x-ray crystallographic screening," *Nat. Biotechnol.*, vol. 18, pp. 1105–1108, 2000.

[4] A. Georgiev, P. K. Allen, and Y. Mezouar, "Microrobotic crystal mounting using computer vision," in *Proc. Microrobotics for Bionanipulation Workshop at IROS'03*, October 2003.

[5] S. Hutchinson, G. Hager, and P. Corke, "A tutorial on visual servo control," *IEEE Trans. on Robotics and Automation*, vol. 12, no. 5, pp. 651–670, October 1996.

[6] P. K. Allen, A. Timcenko, Y. B., and P. Michelman, "Automated tracking and grasping of a moving object with a robotic hand-eye system," *IEEE Trans. on Robotics and Automation*, vol. 9, no. 2, pp. 152–165, April 1993.

[7] J. T. Feddema and T. R. Christenson, "Parallel assembly of high aspect ratio microstructures," in *SPIE Conference on Microrobotics and Micromanipulation*, Boston, USA, September 1999, pp. 153–164.

[8] B. J. Nelson, Y. Zhou, and B. Vikramaditya, "Sensor-based microassembly of hybrid mems devices," *IEEE J. of Control System*, pp. 35–45, December 1998.

[9] S. Yu and B. J. Nelson, "Autonomous injection of biological cells using visual servoing," *The International Journal of Robotics Research (IJRR)*, vol. 21, no. 10-11, pp. 861–868, October-November 2002.

[10] K. Hashimoto, *Visual Servoing : Real Time Control of Robot Manipulators Based on Visual Sensory Feedback*. World Scientific Series in Robotics and Automated Systems, Vol 7, World Scientific Press, Singapor, 1993.

[11] L. Weiss, A. Sanderson, and C. Neuman, "Dynamic sensor-based control of robots with visual feedback," *IEEE Journal of Robotics and Automation*, vol. 3, no. 5, pp. 404–417, October 1987.

[12] P. Martinet, N. Daucher, J. Gallice, and M. Dhome, *Robot control using monocular pose estimation*. Worshop on New Trends in Image-based Robot Servoing, IROS'97, Grenoble, 1997.

[13] W. Wilson, C. W. Hulls, and G. Bell, "Relative end-effector control using cartesian position-based visual servoing," *IEEE Trans. on Robotics and Automation*, vol. 12, no. 5, pp. 684–696, 1996.

[14] F. Chaumette, "Potential problems of stability and convergence in image-based and position-based visual servoing," *The Confluence of Vision and Control, D. Kriegman, G. Hager, A. Morse (eds), LNCIS Series, Springer Verlag*, vol. 237, pp. 66–78, 1998.

[15] H.-Y. Chan and W. J. Li, "A thermally actuated polymer micro robotic gripper for manipulation of biological cells," in *Proc. IEEE International Conference on Robotics and Automation*, September 2003, pp. 288–293.

[16] F. Arai, T. Sakami, H. Maruyama, A. Ichikawa, and T. Fukuda, "Minimally invasive micromanipulation of microbe by laser trapped micro tools," in *Proc. IEEE International Conference on Robotics and Automation*, Washington, DC, May 2002, pp. 1937–1942.

[17] S. Haliyo, S. Regnier, and J.-C. Guinot, "[mü]mad, the adhesion based dynamic micro-manipulator," *European Journal of Mechanics - A/Solids*, vol. 22, no. 6, pp. 903–916, November 2003.

[18] G. Flandin, F. Chaumette, and E. Marchand, "Eye-in-hand / eye-to-hand cooperation for visual servoing," in *IEEE Int. Conf. on Robotics and Automation*, San Francisco, CA, April 2000.

[19] G. Hager and P. Belhumeur, "Efficient region tracking with parametric models of geometry and illumination," *PAMI*, vol. 20, no. 10, pp. 1025–1039, October 1998.

[20] Y. Mezouar and P. K. Allen, "Visual servoed micropositioning for protein manipulation," in *Int. Conf. Intelligent Robots and Systems, Lausanne, Switzerland*, 2002, pp. 1766–1771.